

Training on Synthetic Data Beats Real Data in Multimodal Relation Extraction

Zilin Du, Haoxin Li, Xu Guo, Boyang Li
Nanyang Technological University
Singapore

{zilin003, haoxin003, xu008, boyang.li}@ntu.edu.sg

Abstract

The task of multimodal relation extraction has attracted significant research attention, but progress is constrained by the scarcity of available training data. One natural thought is to extend existing datasets with cross-modal generative models. In this paper, we consider a novel problem setting, where only unimodal data, either text or image, are available during training. We aim to train a multimodal classifier from synthetic data that perform well on real multimodal test data. However, training with synthetic data suffers from two obstacles: lack of data diversity and label information loss. To alleviate the issues, we propose Mutual Information-aware Multimodal Iterated Relational dAta GEneration (MI²RAGE), which applies Chained Cross-modal Generation (CCG) to promote diversity in the generated data and exploits a teacher network to select valuable training samples with high mutual information with the ground-truth labels. Comparing our method to direct training on synthetic data, we observed a significant improvement of 24.06% F1 with synthetic text and 26.42% F1 with synthetic images. Notably, our best model trained on completely synthetic images outperforms prior state-of-the-art models trained on real multimodal data by a margin of 3.76% in F1. Our codebase will be made available upon acceptance.

1. Introduction

Relation extraction (RE) [15, 44, 78, 80, 88] aims to categorize relationships between two entities. Recently, there has been significant interest in multimodal relation extraction (MRE) [6, 8, 11, 30, 43, 93, 95]. Compared to text-only relation extraction, MRE offers the advantages of reduced ambiguity and enhanced representation learning by utilizing complementary bimodal features. However, advances in MRE are hindered by data scarcity, partially due to the difficulty of collecting well-aligned multimodal data. For example, the popular MNRE-2 dataset [95] contains 15,485 data samples in only 23 relation types. In contrast, sev-

eral textual RE datasets, such as WebNLG [19], WikiReading [23], and FewRel [18], possess more than 100 relation classes and up to millions of data instances.

To handle data scarcity in MRE, a natural thought is to complement unimodal training data with synthetic data to create multimodal training data, since text-to-image generative models [4, 12, 26, 35, 58, 59, 61, 90] and image-to-text captioning models [1, 39, 45, 46, 64, 72, 75, 91] have made impressive stride recently. To investigate the feasibility of this approach, we consider a new problem, Multimodal Relation Extraction with a Missing Modality, where we artificially remove one modality from the training data. We train a multimodal network using real data in one modality and synthetic data in the other. During inference, we use real data from both modalities, if they are available.

However, training neural networks with synthetic data is fraught with challenges. In this paper, we identify and tackle two, namely the lack of data diversity and label information loss. The first challenge, the lack of diversity, is caused by the fact that generative models tend to over-represent high-frequency content [22, 62], leading to suppressed tails of the data distribution. This is also observable in Fig. 1, where the generated images appear rather similar. To alleviate this issue, we propose Chained Cross-modal Generation, where we chain and repeatedly apply text-to-image and image-to-text generators. For example, we first generate some text from synthetic images, and generate images on the resulting text. Each generation step introduces some variance to the generated data and enhances diversity.

Another obstacle is that, synthetic data, especially after repeated Chained Cross-modal Generation, may lose information about the data label. We refer to this issue as label information loss. Some examples are given in Fig. 1 (a) and (e), where the synthetic image becomes unrelated to the relation label *Awarded*. To handle the issue, we train a (mostly) unimodal teacher network to predict the label from the synthetic modality only. After that, we keep only data instances with low training losses, which are then used either as input to the next chained generation round or as training data for a multimodal student network (See Fig.



Real View & Entity Pair	Synthetic Views	Relation Label
<p>The year is 2038. 58 year old Rafa Nadal has won The French Open again.</p>	 <p>(a) ✗ (b) (c) (d) (e) ✗</p>	Awarded
 <p>"Piolo Pascual" "Arci Munoz"</p>	<p>(f) a couple sitting next to each other kissing on a table (g) two people and one is on a cell phone ✗ (h) woman making public appearance in her class, kissing boyfriend (i) a woman sitting next to a man in a restaurant ✗ (j) a young woman who is sitting next to a man who is kissing her cheek</p>	Couple

Figure 1. Examples of synthetic data from cross-modality generative models. The first row is image generation, while the second row is image captioning. The samples marked by ✗ are unrelated to the relation label.

2). This process can be understood as identifying synthetic data with high mutual information with ground-truth labels (see detailed discussion in §3.1), which are intuitively good data for training [25, 68].

We propose Mutual Information-aware Multimodal Iterated Relational dAta GEneration (MI²RAGE), which iteratively applies cross-modal generators to create a rich and diverse multimodal training set and exploits a teacher network to select valuable training samples with high mutual information with the ground-truth labels. Our contributions can be summarized as follows.

- We investigate a novel and challenging variation of multimodal relation extraction where, during training, data from one modality are inaccessible and must be synthesized using cross-modal generation.
- We propose to chain text-to-image and image-to-text generators in order to enhance data diversity and employ a teacher network to select training samples with low training losses. From an information-theoretical perspective, we justify the teacher network as selecting synthetic data that are informative about the label.
- Our best model, trained on real text and synthetic images, sets a new state of the art on MNRE-2 and outperforms the best baseline, TMR [96], by 3.76% in F1, even though TMR was trained on both real and synthetic data in both modalities. An ablation study reveals that the proposed technique surpasses naive synthetic data baselines by a massive 24.28-26.52% margin in F1 score.

2. Problem Definition

Multimodal relation extraction begins with a text snippet, which contains textual references to two entities, and an image. Between the entities, it is necessary to differentiate

between the *subject* and the *object*, as the relation between them may be unidirectional (e.g., Above, Eat). An example subject-relation-object tuple is (Yoda, Present-in, Last Jedi). Given the input, the task is to predict the exact relation between the two entities, but they may also be unrelated.

In this paper, we propose a new problem formulation, Multimodal Relation Extraction with a Missing Modality (MREMM), in which data from one modality are inaccessible during training. Specifically, we investigate two settings: *Without Real Texts* and *Without Real Images*. Nevertheless, we need to learn a multimodal relation classifier. For simplicity, we often refer to the text snippet and the corresponding image as the two *views* within the same data instance. One possible solution to MREMM is to synthesize the missing view from the available view, and use both as training data.

3. Method

Fig. 2 illustrates the overall procedure of MI²RAGE. In the MREMM problem, we start with real training data from either the text or image modality, which is referred to as U_0 . After we feed U_0 to the cross-modal generator, we acquire a set of synthetic views called V'_0 . Note that we may generate several synthetic views for each real view. The cross-modal generator from U_0 to V'_0 is denoted as $\mathcal{G}_{U \rightarrow V}$ and the generator in the reverse direction is denoted as $\mathcal{G}_{V \rightarrow U}$.

To select informative training data, we construct a teacher network that learns to predict the ground-truth label from the synthetic view *only*. Note that, in V'_0 , each synthetic view is created from one real view and is thus associated with a ground-truth label. When the synthetic data are images, we also feed the entity names to the network, so

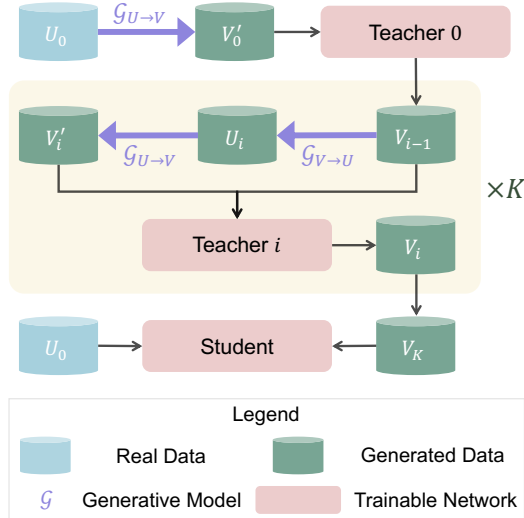


Figure 2. Overview of MI²RAGE. U denotes real data in one modality (text or imagery) and V denotes synthetic data in the other modality. Starting from real data U_0 , we iteratively apply generative networks $\mathcal{G}_{U \rightarrow V}$ and $\mathcal{G}_{V \rightarrow U}$ to generate a series of synthetic datasets V_i . We train teacher networks to select informative training data. The student network is trained with the real views U_0 and the selected synthetic views V_K .

that the network knows which entity pair the relation is for. From all synthetic data, we select those with low training losses, yielding a new dataset V_0 . We argue that the teacher network helps to select training data with high mutual information with the ground-truth label and guard against semantic drift. See analysis in §3.1.

Instead of stopping at V_0 , we apply another round of cross-modal generation; we apply $\mathcal{G}_{V \rightarrow U}$ on V_0 and create U_1 , which is then fed to $\mathcal{G}_{U \rightarrow V}$ to produce V'_1 . We then train another teacher network on $V'_1 \cup V_0$ to once again remove data points with high training loss. This process (yellow box in Fig. 2) can be repeated K times. We name this recursive generation Chained Cross-modal Generation. Finally, we combine the synthetic views V_K and the real views U_0 as training data for the student network.

3.1. Why the Teacher Networks

We justify the teacher networks from an information-theoretic perspective. With abuse of notation, we denote the real view (either text or image) as random variable U , and the synthetic view as random variable V . The class label is denoted as Y . The real-world data distributions are $P(\cdot)$ and the synthetic data distributions are $Q(\cdot)$. Note the off-the-shelf pretrained generator $\mathcal{G}_{U \rightarrow V}$ takes only U as input and not the class label Y . Therefore, the synthetic data distribution factorizes as $Q(V|U)P(U|Y)$. More generally, as in the proposed Chained Cross-modal Generation, we chain $\mathcal{G}_{U \rightarrow V}$ and $\mathcal{G}_{V \rightarrow U}$ and generate a sequence of syn-

thetic data, $V_1, U_2, V_2, \dots, U_K, V_K$, whose distribution factorizes as

$$P(U_1|Y)Q(V_1|U_1) \prod_{i=2}^K Q(U_i|V_{i-1})Q(V_i|U_i). \quad (1)$$

However, each generation step may lose information of the label Y , so the final V_K may be close to being independent of Y and cannot serve as effective training data. Similar phenomena are sometimes referred to as semantic drift in the NLP literature [92].

To prevent information loss, we aim to choose synthetic training data with high mutual information with the ground-truth labels. It is well known that minimizing the cross-entropy loss can be understood as maximizing mutual information $I(V; Y)$ between network input V and label Y (e.g., [5, 51, 55, 56, 70, 71]).

Proposition 1. *Let V be the input variable, Y be a uniformly distributed discrete label, and $f(v, y) \in \mathbb{R}$ be an arbitrary neural network. The negative cross-entropy loss is a lower bound for the mutual information,*

$$I(V, Y) \geq \mathbb{E}_{V, Y} \left[\log \frac{\exp f(v, y)}{\sum_{y'} [\exp f(v, y')] } \right]. \quad (2)$$

Therefore, to find data with high mutual information with the label, we pick those with low training losses. Further, due to the Markov factorization of Eq. 1, we can prove the following (details in the supplemental material).

Proposition 2. *The mutual information $I(V_K; Y)$ is the lower bound of the mutual information between any pairs of variables on the Markov chain from Y to U_{K-1} :*

$$I(V_K; Y) \leq \min\{I(U_i; Y), I(V_i; Y), I(V_i; U_i), I(U_i; V_{i-1})\} \quad \forall i. \quad (3)$$

Thus, if the teacher network finds V_K with high mutual information with Y , we can ensure the information flows from Y to V_K through all the intermediate variables. On the other hand, if V_i has low mutual information with Y , subsequent generation from V_i cannot recover the information. Hence, we perform data filtering before every CCG iteration to make sure the synthesis of new data is conducted from sound starting positions.

The use of separately trained teacher networks contrasts with some recent studies on synthetic training data [60, 67, 81], which discard text-image pairs with low similarity as determined by the pretrained CLIP model [57]. However, the two views may be similar in aspects unrelated to the label. For example, an image of a person wearing a red t-shirt holding a cup and the text “a person wearing a red t-shirt” may be quite similar, but the text omits the relation between the person and the cup and would have low mutual information with the label Holding.

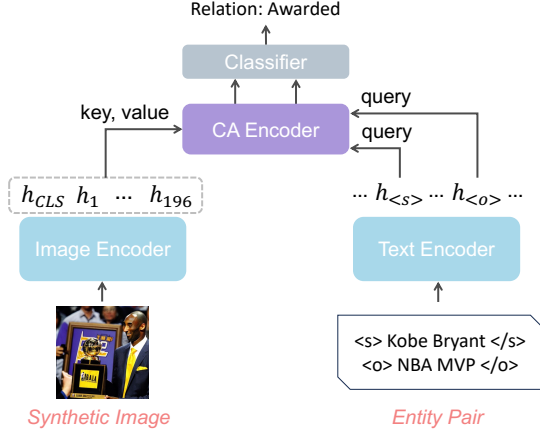


Figure 3. The teacher network for synthetic image selection. As input, the teacher receives only the entities, e.g., the subject Kobe Bryant and the object NBA MVP, and the synthetic image.

3.2. The Teacher Network Architecture

The objective of the teacher network is to select good synthetic data. As a result, we need to constrain its input to the synthetic view as much as possible. Suppose we provide both view to the teacher network, then it could learn to predict the label directly from the real view, which contains ample label information, in complete contradiction of the original purpose of the teacher network.

Before introducing the teacher networks, we first discuss how the entities are encoded. Each entity pair contains a subject and an object. We use special tokens $\langle s \rangle$ and $\langle /s \rangle$ to mark the position of the subject entity and special tokens $\langle o \rangle$ and $\langle /o \rangle$ to mark the object. For example, the two-token subject [New, York] becomes $[\langle s \rangle, \text{New, York}, \langle /s \rangle]$ after the special tokens are added. We then take the representations of the tokens $\langle s \rangle$ and $\langle o \rangle$ from the last encoder layer as the encodings of the subject and the object respectively, which are denoted as $\mathbf{h}_{\langle s \rangle}$ and $\mathbf{h}_{\langle o \rangle}$.

The teacher network responsible for filtering synthetic textual data is a pretrained text-only network, such as BERT. Its input contains a single image caption. We append both entity names at the end to remove any ambiguity since the synthetic captions often do not contain the entity names. A real text snippet, on the contrary, always contains the entity names. At the last layer, we extract the encoded entity vectors ($\mathbf{h}_{\langle s \rangle}$ and $\mathbf{h}_{\langle o \rangle}$ from $\langle s \rangle$ and $\langle o \rangle$), and feed their concatenation into a linear classifier. We finetune all neural network parameters using the cross-entropy loss.

The teacher network for selecting synthetic images is slightly more complex; we show its architecture in Fig. 3. We use a pretrained vision transformer to encode the image, and a pretrained textual encoder to incorporate information from the entities. We limit the input to the textual encoder

to only the entity names, so that the network sees as little textual information as possible. We adopt a cross-attention layer, where the textual representations $\mathbf{h}_{\langle s \rangle}$ and $\mathbf{h}_{\langle o \rangle}$ serve as query vectors, and image patch encodings serve as the keys and values. The results of the cross-attention are two vectors, whose concatenation is input to a linear classifier. We finetune all network parameters.

3.3. The Student Network Architecture

The student network should learn effective multimodal representations from real and synthetic training data. We design a network architecture that exploits a particular strength of training from synthetic data: we can generate as many synthetic views as we want for real view, both at training time and at inference time. Take text-to-image generation for example; each image may be considered as an imaginative interpretation of the text, which enriches the textual representation [48, 66]. As such, we exploit the enrichment during both training and inference.

The model architecture is shown in Fig. 4. We use a cross-attention layer to combine multiple instances in the synthetic modality. Given a query vector \mathbf{q} , a key matrix M_K , and a value matrix M_V , the cross-attention operation can be written as

$$\text{CA}(\mathbf{q}, M_K, M_V) = \sigma \left(\frac{M_K W_K W_Q \mathbf{q}}{\sqrt{d}} \right) (W_V M_V), \quad (4)$$

where $\sigma(\cdot)$ is the softmax operation. W_K , W_Q and W_V are trainable parameters. d is a scaling factor equal to the dimension of $W_Q \mathbf{q}$. As in the original Transformer network, the results of cross-attention go through feedforward layers.

When we process real image and synthetic texts (Fig. 4 (a)), for every image we receive N captions from the teacher network and encode them separately. After that, we collect the subject encodings $\mathbf{h}_{\langle s \rangle}$ from all captions into M^{sub} , and all object encodings $\mathbf{h}_{\langle o \rangle}$ into M^{obj} . We take \mathbf{h}_{CLS} , the representation of the $\langle CLS \rangle$ token from the visual encoder, as the query vector. Applying the same CA operation twice, we have two vectors,

$$\text{CA}(\mathbf{h}_{CLS}, M^{sub}, M^{sub}) \text{ and } \text{CA}(\mathbf{h}_{CLS}, M^{obj}, M^{obj}).$$

The vectors go through the feedforward layers of the Transformer network. Their concatenation then go through a linear classifier.

The case for synthetic images and real text is symmetrical (Fig. 4 (b)). For every text snippet, we acquire N images from the teacher network, and encode them separately. After that, we take \mathbf{h}_{CLS} of each image and arrange them into a matrix M^{img} . We take the entity representations $\mathbf{h}_{\langle s \rangle}$ and $\mathbf{h}_{\langle o \rangle}$ and use them as two query vectors. Again, we apply the CA operation twice and obtain two vectors,

$$\text{CA}(\mathbf{h}_{\langle s \rangle}, M^{img}, M^{img}) \text{ and } \text{CA}(\mathbf{h}_{\langle o \rangle}, M^{img}, M^{img}),$$

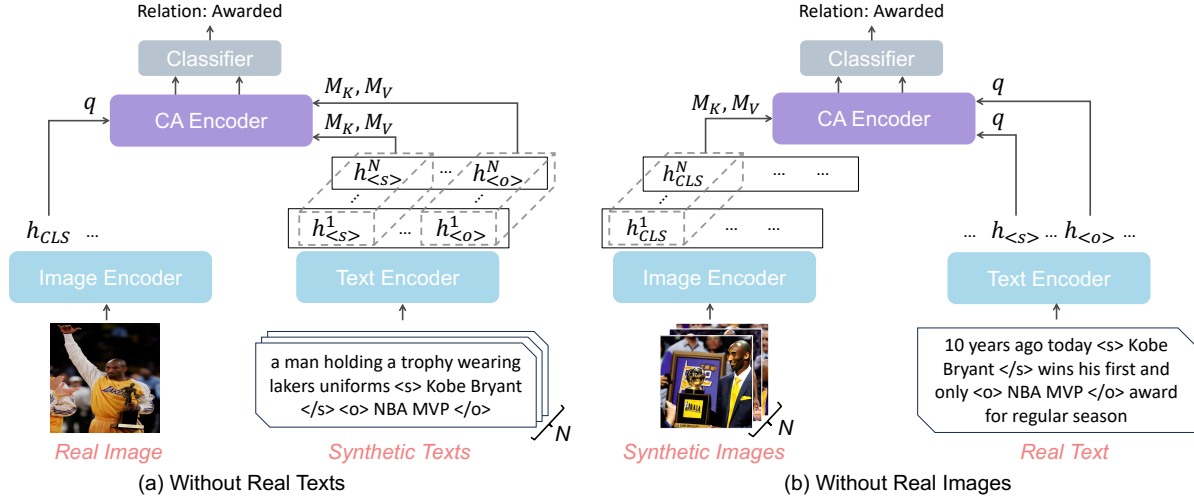


Figure 4. The student networks that predict the relation for an entity pair using real data from one modality and synthetic data from the other. (a) The student that is trained with a real image and N synthetic texts. (b) The student that is trained with a real text snippet and N synthetic images.

which are concatenated and input to subsequent Transformer layers and eventually to a linear classifier. The loss for both student networks is the cross-entropy loss.

During inference, a test data instance contains two views and both are real. In order to fully realize the strength of data synthesis, we still generate a number of new views in the synthetic modality. Using the trained teacher network, we select N synthetic views with the lowest losses. After that, we append the real view in the synthetic modality to the synthetic views, and feed all available views to the student network. This process is reminiscent of the technique of inference-time data augmentation.

3.4. Why Chained Cross-modal Generation

To maximize the benefits from synthetic training data, they should be as similar to genuine data as possible. However, the synthetic data may exhibit significant differences from the real data. In particular, existing research [22, 62] suggests they may over-represent high-frequency content and have thinner tails than the real distribution. This phenomenon is also observable in the generated images in Fig. 1, which have similar backgrounds.

We present a simple analysis of distribution similarity from the perspective of Monte Carlo expectation. The empirical negative cross-entropy can be understood as a Monte Carlo approximation for expectation,

$$\frac{1}{N} \sum_{y,v} \log P_{\theta}(Y = y|V = v) \approx \mathbb{E}_{P(V,Y)}[\log P_{\theta}(Y|V)], \quad (5)$$

where $P_{\theta}(\cdot)$ denotes the prediction of a network parameterized by θ , N is the total number of data points, and v

and y are drawn from the ground-truth distribution $P(V, Y)$. However, in practice v and y are drawn from the synthetic distribution $Q(V, Y)$. By importance sampling, we have

$$\mathbb{E}[\log P_{\theta}(Y|V)] \approx \frac{1}{N} \sum_{y,v} \frac{P(Y|V)P(V)}{Q(Y|V)Q(V)} \log P_{\theta}(y|v). \quad (6)$$

It is difficult to estimate $P(V, Y)$ and $Q(V, Y)$ and directly apply Eq. 6. Instead, we stick with the simple empirical cross-entropy loss, which works well only when $Q(Y|V)Q(V) \approx P(Y|V)P(V)$. In this paper, we encourage the similarity of $P(V)$ and $Q(V)$ using the CCG technique for sampling V . As each cross-modal generation step introduces some noise, chaining multiple generators likely results in diverse output.

4. Experiments

Dataset. We use the MNRE-2 dataset [95]¹ in our experiments. It contains 15,484 samples within 9,201 image-caption pairs crawled from Twitter. There are 23 relation types including None. Following previous works, we split the dataset into training, validation and testing set with 12247, 1624 and 1614 samples, respectively. Meanwhile, we report the standard micro precision, recall and F1 score for evaluation.

Implementation Details. The text-to-image generator is Stable Diffusion v2.1 [59] with 512×512 resolution, 50 denoising steps, and a guidance scale of 7.5. We use BLIP ViT-L [38] as the image-to-text generator and set p to 0.8

¹<https://github.com/thecharm/MNRE>

in nucleus (top- p) sampling [27]. For both the teacher and the student networks, the text encoder is a pretrained BERT-base and the vision encoder is CLIP ViT-B/16. The cross-attention module is a Transformer layer identical to BERT-base in architecture.

The number of CCG iterations, K , is set to 2. For each real view in U_0 , we first generate 30 synthetic views for V'_0 . The teacher network selects 60%, which is equivalent to 18 views. The first CCG round generates 72 synthetic views, or 4 new views for each input. From the total of $90=18+72$ views, another 60% or 54 views are selected. The second CCG round generates another 54 views. Finally, we select 6 synthetic images for each real text and 10 captions for each real images for training the students. The number of selected synthetic views is determined on the validation set. At test time, we use the same generative procedure to produce synthetic views for each test instance. Further details are available in the supplementary.

Baselines. We compare our methods with 19 baselines, all of which are trained on the real multimodal data. [29, 96] also leverage additional paired image-caption datasets, while [30, 73] retrieve extra images and texts for training. For all baseline performance, we take the reported numbers from their respective paper directly. Details of the baselines can be found in the supplementary.

4.1. Main Results

Table 1 compares MI²RAGE with the baselines. Even though models trained on synthetic data are at an inherent disadvantage, our best model surpasses the best baseline, TMR [96], by 3.76% in F1 and the second best baseline, RECK [14], by 3.97% in F1 and 1.54% in accuracy. Our model trained on synthetic text and real images also performs well, beating every baseline except for TMR and RECK in F1. In accuracy, this model snatches the third position, among all baselines that report this metric.

We observe a performance gap between the synthetic image condition and the synthetic text condition. Based on our observation, we propose two hypothetical reasons. First, there is a distribution gap between synthetic text and real text. In a real text snippet, the entity names are part of the text and serve syntactic functions. However, the synthetic captions rarely contain the entity names, so we need to artificially append the entity names, creating a domain shift that may hurt generalization. Second, the images in MNRE-2 are sometimes semantically misaligned with the text, which is well aligned with the label. Thus, synthetic text may deviate from the label and the real text more than synthetic images deviate from the label and the real images.

4.2. Ablation Study

We create the following ablated versions of MI²RAGE from the $K = 1$ condition: (1) No CCG. This is equiv-

Table 1. Main results on multimodal relation extraction.

Method	Accuracy	Precision	Recall	F1
VBERT [41]	73.97	57.15	59.48	58.30
BSG [95]	77.15	62.95	62.65	62.80
UMT [85]	77.84	62.93	63.88	63.46
UMGF [89]	79.27	64.38	66.23	65.29
MEGA [94]	80.05	64.51	68.44	66.41
MoRe [73]	79.87	65.25	67.32	66.27
GPT4-XMLR [6]	-	-	-	74.56
DGF-PT [43]	79.82	79.72	78.63	79.24
Iformer [40]	92.38	82.59	80.78	81.67
HVPnet [9]	92.52	82.64	80.78	81.85
TSVFN [93]	92.67	85.16	82.07	83.02
MMIB [11]	-	83.49	82.97	83.23
MRE-ISE [77]	94.06	84.69	83.38	84.03
I ² SRM [31]	-	84.65	83.59	84.12
VisualPT-MoE [79]	-	84.81	83.75	84.28
[30]	93.54	85.03	84.25	84.64
[29]	-	84.95	85.76	84.86
RECK [14]	95.11	88.77	<u>88.91</u>	88.84
TMR [96]	-	90.48	87.66	89.05
<i>Without Real Texts</i>				
MI ² RAGE ($K = 1$)	92.63	87.48	84.06	85.74
MI ² RAGE ($K = 2$)	93.60	87.92	84.96	86.42
<i>Without Real Images</i>				
MI ² RAGE ($K = 1$)	<u>95.42</u>	<u>93.74</u>	<u>88.91</u>	<u>91.26</u>
MI ² RAGE ($K = 2$)	96.65	93.92	91.72	92.81

Table 2. An ablation study of MI²RAGE on the MRNE-2 dataset.

Method	Accuracy	Precision	Recall	F1
<i>Without Real Texts</i>				
Ours	92.63	87.48	84.06	85.74
No CCG	81.54	71.61	70.94	71.27
CLIP Teacher	72.12	61.50	56.41	58.84
Random Teacher	73.36	60.89	62.03	61.46
No Teacher	73.54	62.12	61.25	61.68
Unimodal	73.42	63.78	55.31	59.25
<i>Without Real Images</i>				
Ours	95.42	93.74	88.91	91.26
No CCG	78.75	69.77	69.72	68.21
CLIP Teacher	75.40	66.37	58.59	62.24
Random Teacher	75.71	64.79	64.69	64.74
No Teacher	76.21	62.83	66.97	64.84
Unimodal	74.42	58.58	60.25	59.40

alent to setting $K = 0$ and stopping the synthesis at V_0 . (2) CLIP teacher. It replaces our teacher network with a CLIP teacher, which selects synthetic views with the highest CLIP similarity with the corresponding real views and use the result as training data. Every other aspect is the same as MI²RAGE. (3) Random Teacher. It selects syn-

thetic views randomly as training data. (4) No Teacher, which uses all synthetic data indiscriminately to train the student. (5) Unimodal, where only the real views are used in training.

We show the results in Table 2 and make the following observations. First, synthetic data provide enormous benefits. Comparing with using only unimodal data for training, MI²RAGE boosts performance by approximately 20% in accuracy and 30% in F1 across both settings. The results convincingly demonstrate that sometimes training data can make all the difference in model performance. Second, the teacher plays a key role. Our teacher network beats the CLIP teacher by 26.90-29.02% and the random teacher by 24.28-26.52%. Surprisingly, the CLIP teacher does not perform better than the random teacher. This result highlights the importance of filtering synthetic data based on their mutual information with the label as compared to filtering based on CLIP similarity. Third, CCG by itself contributes over 10% improvements in accuracy and F1. Together with Tab. 1, we observe that increasing K is generally beneficial, despite the diminishing marginal effect sizes. As discussed in §3.4, one possible reason may be that CCG increases the diversity of the synthetic data.

4.3. Number of Synthetic Views in Student

The design of the student network exploits multiple synthetic views per real view, in a manner similar to test-time data augmentation. We investigate how the number of synthetic views used during training and test affects the overall accuracy and F1 score.

The top row of Fig. 5 shows the result when training on a varying number of synthetic views. During inference, we use the exact same number of synthetic views to minimize any distribution shift. We observe an inverse U-shape, where the performance increases to a point (6 synthetic images and 12 synthetic text snippets) and then decreases. Performance tends to be low when only 2-4 synthetic views are used, suggesting the potential of synthetic data is not fully realized if insufficient number of views are utilized in training.

After training completes, at test time we also vary the number of synthetic views that we create from each test data point. The results are shown on the bottom row of Fig. 5. We observe similar trends as the top row. Since each synthetic view is a possible interpretation of the real view, a sufficient number of synthetic views may increase the probability that at least one interpretation is correct and correlates well with the label.

4.4. Diversity Estimates

We aim to verify if CCG indeed improves data diversity, as conjectured in §3.4. However, data diversity is inherently difficult to define because simple statistics may not correspond well to semantic diversity. As an approximate mea-

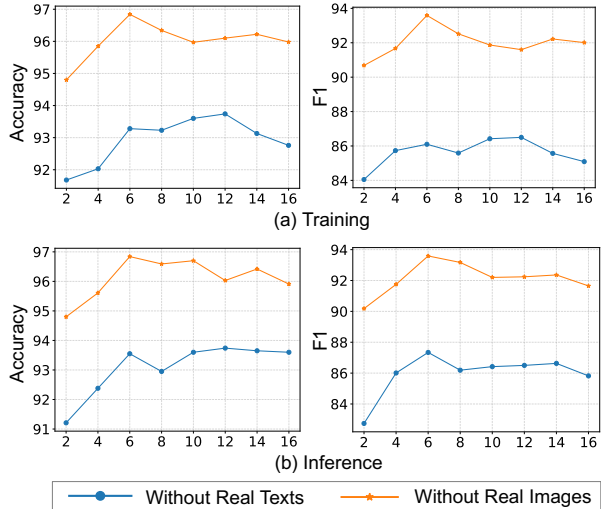


Figure 5. Accuracy and F1 on MNRE-2 as the number of synthetic views used by the student network is varied.

Table 3. Evaluation of the diversity on various synthetic sets.

	V_0	V'_1	V_1	V'_2
Image	6.95×10^{21}	7.37×10^{21}	5.52×10^{21}	7.37×10^{21}
Text	1.85×10^{32}	3.28×10^{32}	3.04×10^{32}	3.71×10^{32}

sure, we use the generalized variance of a Gaussian mixture model (GMM) fitted on synthetic data. First, we extract feature vectors using the original CLIP-ViT-B-32 for synthetic images and BERT-base-uncased for captions. After that, as the data lie in a low-dimensional manifold, we perform dimensionality reduction using principal component analysis. We then fit a 3-component GMM and calculate the generalized variance. We present the variances in Table 3. Each generation step (*i.e.*, $V_0 \rightarrow V'_1$ and $V_1 \rightarrow V'_2$) increases variance, suggesting that CCG enhances data diversity. More details and discussions are in the supplementary.

4.5. Extension to the Textual Dataset WebNLG

We investigate if MI²RAGE can successfully work with a textual relation extraction dataset with a large number of relations. We adopt the WebNLG dataset [19], a text-only relation extraction dataset comprising 171 relation types. Like in MNRE-2, we aim to identify relation types of given entity pairs, rather than identifying the entities.

The results are presented in Table 4. Under this setting, our method continues to surpass unimodal training by 5.24% in F1, highlighting the effectiveness of synthetic multimodal training. In addition, both the teacher model and CCG exhibit performance improvements. However, the performance gains in this setting are not as pronounced as those in multimodal settings (See Table 2).

Table 4. Extension to Textual Dataset WebNLG

Method	Accuracy	Precision	Recall	F1
Ours	98.93	94.86	95.64	95.12
No CCG	97.36	92.81	93.98	93.39
CLIP Teacher	96.35	89.89	90.52	90.20
Random Teacher	96.61	90.75	90.84	90.79
No Teacher	96.48	90.76	91.32	91.04
Unimodal	96.54	89.71	90.05	89.88

We hypothesize that the textual data in WebNLG may be less easy to visualize than the multimodal dataset MNRE-2, leading to a smaller advantage of multimodal classifier. For example, WebNLG contains relations such as `yearOfConstruction` and `postalCode`, which are difficult to visualize. Nevertheless, MI²RAGE still demonstrates higher performance than a pure unimodal approach. Further, the proposed CCG technique and teacher networks both contribute positively.

5. Related Work

Multimodal Relation Extraction. Recent studies on multimodal relation extraction (MRE) [6, 8, 9, 11, 16, 29, 30, 40, 43, 73, 77, 85, 87, 89, 93–95] have demonstrated significant progresses. A common approach is to utilize scene graphs [77, 87, 94], which provide structured information about the image. However, [40] points out that coarse-grained alignment of scene graphs may not effectively utilize visual guidance. Therefore, to establish fine-grained correspondence between images and texts, [31, 40, 43] align tokens in texts with visual objects. To mitigate vagueness and misleadingness in relations, [6] elicits multi-grain textual knowledge from large language models; [30, 73] retrieve relevant texts and images from Internet knowledge corpus (*e.g.*, Wikipedia). Additionally, RECK [14] leverages ConceptNet to extract conceptual relations.

TMR [96] is the only existing work that makes use of text-to-image generation in MRE. In the ablation study of TMR, the synthetic data accounts for about 2.68% gains in F1, which roughly matches our experiments when no data filtering by the teacher network is performed (Table 2). The teacher network of MI²RAGE leads to significant performance boosts in addition to that.

In contrast to prior works that train on well-aligned multimodal data, we investigate a new problem, Multimodal Relation Extraction with a Missing Modality, where data from one modality (image or text) are inaccessible during training.

Training with Synthetic Data. Building off image generation and image captioning, training on synthetic data has emerged as a promising research direction [34, 54]. In com-

puter vision, [24, 33, 69] explore the use of synthetic data in object detection; [3, 84] demonstrate benefits of complementing real images with synthetic images as training data. In language tasks, research examines the generation of additional textual training data [17, 28, 52, 53, 74, 76, 83]. The pioneering work Vokenization [66] proposes that language tasks can benefit from visualization of textual tokens, but builds the visualizations through retrieval rather than synthesis. The idea has been extended by researchers synthesizing visual data conditioned on the text for applications such as machine translation [20, 47], story generation [97], procedural planning [49], dialogue summarization [67] and low-resource language understanding [48, 81]. In long sequence understanding tasks, VCoT [60] generates both images and texts at intermediate states to bridge semantic gaps between two specified states.

Differing from previous approaches that target unimodal tasks, [13] target multimodal event extraction and generative images from text and vice versa. In this work, we extend direct bidirectional generation to iterating through the text-to-image generator and the image-to-text generator multiple times.

Learning from Noisy Data. Noise in training data is a common phenomenon. Many works investigate the issue of label noise, where training data samples are associated with incorrect labels. Theoretical analysis [42] and empirical observation [2, 65] support the notion that DNNs learn generalizable patterns first and gradually overfit to noisy patterns. Therefore, it is common to select data samples with low training loss in subsequent rounds of training [7, 63, 82]. To reduce confirmation bias, [21, 36, 50, 86] simultaneously train two networks and combine their predictions to identify clean labels. MentorNet [32] learns a curriculum that selects training data for a student network. In another line of research, [37] proposes to handle data noise in the form of corrupted and out-of-distribution inputs.

The use of one neural network to select training data for another [21, 32] bears resemblance to our approach. However, in our problem setting, the labels are assumed to be always correct. The purpose of our teacher network is to prevent gradual loss of label information in the synthetic data rather than identifying incorrect labels.

6. Conclusions

This paper introduces a new problem in Multimodal Relation Extraction: only unimodal data (either text or image) is available during training and we need to generate data for the missing modality to train a MRE classifier. To tackle this problem, we propose the Mutual Information-aware Multimodal Iterated Relational dAta GEneration (MI²RAGE) approach that comprises two procedures. Chained Cross-modal Generation promotes data diversity by repeatedly applying the text-to-image and

image-to-text generators. To mitigate the label information loss, MI²RAGE selects synthetic training data that have higher mutual information with the ground-truth labels. Experiments on the MNRE-2 benchmark demonstrate that the MRE classifier trained using the synthetic data generated by MI²RAGE outperforms state-of-the-art models trained on real multimodal data on the real multimodal test set. Ablation studies further underscore the effectiveness of each component in MI²RAGE. Additionally, MI²RAGE exhibits performance gains in traditional text-only relation extraction by converting unimodal training data to multimodal data. We believe MI²RAGE opens new avenues to the MRE problem and training on synthetic data in general.

References

- [1] Jean-Baptiste Alayrac, Jeff Donahue, Pauline Luc, Antoine Miech, Iain Barr, Yana Hasson, Karel Lenc, Arthur Mensch, Katherine Millican, Malcolm Reynolds, et al. Flamingo: a visual language model for few-shot learning. *Advances in Neural Information Processing Systems*, 35:23716–23736, 2022. [1](#)
- [2] Devansh Arpit, Stanislaw Jastrzebski, Nicolas Ballas, David Krueger, Emmanuel Bengio, Maxinder S Kanwal, Tegan Maharaj, Asja Fischer, Aaron Courville, Yoshua Bengio, et al. A closer look at memorization in deep networks. In *International conference on machine learning*, pages 233–242. PMLR, 2017. [8](#)
- [3] Shekoofeh Azizi, Simon Kornblith, Chitwan Saharia, Mohammad Norouzi, and David J. Fleet. Synthetic data from diffusion models improves imagenet classification. *arXiv Preprint 2304.08466*, 2023. [8](#)
- [4] Yogesh Balaji, Seungjun Nah, Xun Huang, Arash Vahdat, Jiaming Song, Karsten Kreis, Miika Aittala, Timo Aila, Samuli Laine, Bryan Catanzaro, et al. ediffi: Text-to-image diffusion models with an ensemble of expert denoisers. *arXiv preprint arXiv:2211.01324*, 2022. [1](#)
- [5] Malik Boudiaf, Jérôme Rony, Imtiaz Masud Ziko, Eric Granger, Marco Pedersoli, Pablo Piantanida, and Ismail Ben Ayed. A unifying mutual information view of metric learning: Cross-entropy vs. pairwise losses. In *Computer Vision – ECCV 2020*, pages 548–564, Cham, 2020. Springer International Publishing. [3](#)
- [6] Feng Chen and Yujian Feng. Chain-of-thought prompt distillation for multimodal named entity and multimodal relation extraction. *arXiv preprint arXiv:2306.14122*, 2023. [1](#), [6](#), [8](#), [3](#)
- [7] Pengfei Chen, Ben Ben Liao, Guangyong Chen, and Shengyu Zhang. Understanding and utilizing deep neural networks trained with noisy labels. In *International Conference on Machine Learning*, pages 1062–1070. PMLR, 2019. [8](#)
- [8] Qiang Chen, Dong Zhang, Shoushan Li, and Guodong Zhou. A unified mrc framework with multi-query for multi-modal relation triplets extraction. In *2023 IEEE International Conference on Multimedia and Expo (ICME)*, pages 552–557. IEEE, 2023. [1](#), [8](#)
- [9] Xiang Chen, Ningyu Zhang, Lei Li, Yunzhi Yao, Shumin Deng, Chuanqi Tan, Fei Huang, Luo Si, and Huajun Chen. Good visual guidance make a better extractor: Hierarchical visual prefix for multimodal entity and relation extraction. In *Findings of the Association for Computational Linguistics: NAACL 2022*, pages 1607–1618, 2022. [6](#), [8](#), [3](#)
- [10] Ekin D Cubuk, Barret Zoph, Jonathon Shlens, and Quoc V Le. Randaugment: Practical automated data augmentation with a reduced search space. In *Proceedings of the IEEE/CVF conference on computer vision and pattern recognition workshops*, pages 702–703, 2020. [2](#), [3](#)
- [11] Shiyao Cui, Jiangxia Cao, Xin Cong, Jiawei Sheng, Quanguang Li, Tingwen Liu, and Jinqiao Shi. Enhancing multimodal entity and relation extraction with variational information bottleneck. *arXiv preprint arXiv:2304.02328*, 2023. [1](#), [6](#), [8](#)
- [12] Xiaoliang Dai, Ji Hou, Chih-Yao Ma, Sam Tsai, Jialiang Wang, Rui Wang, Peizhao Zhang, Simon Vandenhende, Xiaofang Wang, Abhimanyu Dubey, Matthew Yu, Abhishek Kadian, Filip Radenovic, Dhruv Mahajan, Kunpeng Li, Yue Zhao, Vladan Petrovic, Mitesh Kumar Singh, Simran Motwani, Yi Wen, Yiwen Song, Roshan Sumbaly, Vignesh Ramanathan, Zijian He, Peter Vajda, and Devi Parikh. Emu: Enhancing image generation models using photogenic needles in a haystack. *arXiv Preprint 2309.15807*, 2023. [1](#)
- [13] Zilin Du, Yunxin Li, Xu Guo, Yidan Sun, and Boyang Li. Training multimedia event extraction with generated images and captions. *arXiv preprint arXiv:2306.08966*, 2023. [8](#)
- [14] Junhao Feng, Guohua Wang, Changmeng Zheng, Yi Cai, Ze Fu, Yaowei Wang, Xiao-Yong Wei, and Qing Li. Towards bridged vision and language: Learning cross-modal knowledge representation for relation extraction. *IEEE Transactions on Circuits and Systems for Video Technology*, 2023. [6](#), [8](#), [3](#)
- [15] Tsu-Jui Fu, Peng-Hsuan Li, and Wei-Yun Ma. Graphrel: Modeling text as relational graphs for joint entity and relation extraction. In *Proceedings of the 57th annual meeting of the association for computational linguistics*, pages 1409–1418, 2019. [1](#)
- [16] Ze Fu, Junhao Feng, Changmeng Zheng, and Yi Cai. Knowledge-enhanced scene graph generation with multimodal relation alignment (student abstract). In *Proceedings of the AAAI Conference on Artificial Intelligence*, pages 12947–12948, 2022. [8](#)
- [17] Jiahui Gao, Renjie Pi, LIN Yong, Hang Xu, Jiacheng Ye, Zhiyong Wu, Weizhong Zhang, Xiaodan Liang, Zhenguo Li, and Lingpeng Kong. Self-guided noise-free data generation for efficient zero-shot learning. In *International Conference on Learning Representations*, 2023. [8](#)
- [18] Tianyu Gao, Xu Han, Hao Zhu, Zhiyuan Liu, Peng Li, Maosong Sun, and Jie Zhou. Fewrel 2.0: Towards more challenging few-shot relation classification. In *Proceedings of the 2019 Conference on Empirical Methods in Natural Language Processing and the 9th International Joint Conference on Natural Language Processing (EMNLP-IJCNLP)*, pages 6250–6255, 2019. [1](#)
- [19] Claire Gardent, Anastasia Shimorina, Shashi Narayan, and Laura Perez-Beltrachini. Creating training corpora for nlg

- micro-planners. In *Proceedings of the 55th Annual Meeting of the Association for Computational Linguistics (Volume 1: Long Papers)*, pages 179–188. Association for Computational Linguistics, 2017. 1, 7
- [20] Devaansh Gupta, Siddhant Kharbanda, Jiawei Zhou, Wanhua Li, Hanspeter Pfister, and Donglai Wei. Cliptrans: Transferring visual knowledge with pre-trained models for multimodal machine translation. In *Proceedings of the IEEE/CVF International Conference on Computer Vision*, pages 2875–2886, 2023. 8
- [21] Bo Han, Quanming Yao, Xingrui Yu, Gang Niu, Miao Xu, Weihua Hu, Ivor Tsang, and Masashi Sugiyama. Co-teaching: Robust training of deep neural networks with extremely noisy labels. *Advances in neural information processing systems*, 31, 2018. 8
- [22] Lisa Anne Hendricks, Kaylee Burns, Kate Saenko, Trevor Darrell, and Anna Rohrbach. Women also snowboard: Overcoming bias in captioning models. In *Proceedings of the European Conference on Computer Vision (ECCV)*, 2018. 1, 5
- [23] Daniel Hewlett, Alexandre Lacoste, Llion Jones, Illia Polosukhin, Andrew Fandrianto, Jay Han, Matthew Kelcey, and David Berthelot. Wikireading: A novel large-scale language understanding task over wikipedia. In *Proceedings of the 54th Annual Meeting of the Association for Computational Linguistics (Volume 1: Long Papers)*, pages 1535–1545, 2016. 1
- [24] Stefan Hinterstoisser, Vincent Lepetit, Paul Wohlhart, and Kurt Konolige. On pre-trained image features and synthetic images for deep learning. In *ECCV 2018 Workshops*, 2018. 8
- [25] R Devon Hjelm, Alex Fedorov, Samuel Lavoie-Marchildon, Karan Grewal, Phil Bachman, Adam Trischler, and Yoshua Bengio. Learning deep representations by mutual information estimation and maximization. In *International Conference on Learning Representations*, 2019. 2
- [26] Jonathan Ho, Ajay Jain, and Pieter Abbeel. Denoising diffusion probabilistic models. *Advances in neural information processing systems*, 33:6840–6851, 2020. 1
- [27] Ari Holtzman, Jan Buys, Li Du, Maxwell Forbes, and Yejin Choi. The curious case of neural text degeneration. *arXiv preprint arXiv:1904.09751*, 2019. 6
- [28] Or Honovich, Thomas Scialom, Omer Levy, and Timo Schick. Unnatural instructions: Tuning language models with (almost) no human labor. *arXiv preprint arXiv:2212.09689*, 2022. 8
- [29] Xuming Hu, Junzhe Chen, Aiwei Liu, Shiao Meng, Lijie Wen, and Philip S Yu. Prompt me up: Unleashing the power of alignments for multimodal entity and relation extraction. In *Proceedings of the 31st ACM International Conference on Multimedia*, pages 5185–5194, 2023. 6, 8, 3
- [30] Xuming Hu, Zhijiang Guo, Zhiyang Teng, Irwin King, and Philip S Yu. Multimodal relation extraction with cross-modal retrieval and synthesis. *arXiv preprint arXiv:2305.16166*, 2023. 1, 6, 8, 3
- [31] Yusheng Huang and Zhouhan Lin. I2srm: Intra-and inter-sample relationship modeling for multimodal information extraction. *arXiv preprint arXiv:2310.06326*, 2023. 6, 8, 3
- [32] Lu Jiang, Zhengyuan Zhou, Thomas Leung, Li-Jia Li, and Li Fei-Fei. MentorNet: Learning data-driven curriculum for very deep neural networks on corrupted labels. In *Proceedings of the 35th International Conference on Machine Learning*, pages 2304–2313. PMLR, 2018. 8
- [33] Matthew Johnson-Roberson, Charles Barto, Rounak Mehta, Sharath Nittur Sridhar, Karl Rosaen, and Ram Vasudevan. Driving in the matrix: Can virtual worlds replace human-generated annotations for real world tasks? In *2017 IEEE International Conference on Robotics and Automation (ICRA)*, 2017. 8
- [34] Aman Kishore, Tae Eun Choe, Junghyun Kwon, Minwoo Park, Pengfei Hao, and Akshita Mittel. Synthetic data generation using imitation training. In *Proceedings of the IEEE/CVF International Conference on Computer Vision (ICCV) Workshops*, pages 3078–3086, 2021. 8
- [35] Nupur Kumari, Bingliang Zhang, Richard Zhang, Eli Shechtman, and Jun-Yan Zhu. Multi-concept customization of text-to-image diffusion. In *Proceedings of the IEEE/CVF Conference on Computer Vision and Pattern Recognition*, pages 1931–1941, 2023. 1
- [36] Junnan Li, Richard Socher, and Steven CH Hoi. Dividemix: Learning with noisy labels as semi-supervised learning. *arXiv preprint arXiv:2002.07394*, 2020. 8
- [37] Junnan Li, Caiming Xiong, and Steven CH Hoi. Learning from noisy data with robust representation learning. In *Proceedings of the IEEE/CVF International Conference on Computer Vision*, pages 9485–9494, 2021. 8
- [38] Junnan Li, Dongxu Li, Caiming Xiong, and Steven Hoi. Blip: Bootstrapping language-image pre-training for unified vision-language understanding and generation. In *International Conference on Machine Learning*, pages 12888–12900. PMLR, 2022. 5
- [39] Junnan Li, Dongxu Li, Silvio Savarese, and Steven Hoi. Blip-2: Bootstrapping language-image pre-training with frozen image encoders and large language models. *arXiv preprint arXiv:2301.12597*, 2023. 1
- [40] Lei Li, Xiang Chen, Shuofei Qiao, Feiyu Xiong, Huajun Chen, and Ningyu Zhang. On analyzing the role of image for visual-enhanced relation extraction (student abstract). In *Proceedings of the AAAI Conference on Artificial Intelligence*, pages 16254–16255, 2023. 6, 8, 3
- [41] Liunian Harold Li, Mark Yatskar, Da Yin, Cho-Jui Hsieh, and Kai-Wei Chang. Visualbert: A simple and performant baseline for vision and language. *arXiv preprint arXiv:1908.03557*, 2019. 6
- [42] Mingchen Li, Mahdi Soltanolkotabi, and Samet Oymak. Gradient descent with early stopping is provably robust to label noise for overparameterized neural networks. In *International conference on artificial intelligence and statistics*, pages 4313–4324. PMLR, 2020. 8
- [43] Qian Li, Shu Guo, Cheng Ji, Xutan Peng, Shiyao Cui, and Jianxin Li. Dual-gated fusion with prefix-tuning for multimodal relation extraction. *arXiv preprint arXiv:2306.11020*, 2023. 1, 6, 8, 3

- [44] Xiaoya Li, Fan Yin, Zijun Sun, Xiayu Li, Arianna Yuan, Duo Chai, Mingxin Zhou, and Jiwei Li. Entity-relation extraction as multi-turn question answering. In *Proceedings of the 57th Annual Meeting of the Association for Computational Linguistics*, pages 1340–1350, 2019. 1
- [45] Xiujun Li, Xi Yin, Chunyuan Li, Pengchuan Zhang, Xiaowei Hu, Lei Zhang, Lijuan Wang, Houdong Hu, Li Dong, Furu Wei, Yejin Choi, and Jianfeng Gao. Oscar: Object-semantic aligned pre-training for vision-language tasks. In *ECCV 2020*, 2020. 1
- [46] Haotian Liu, Chunyuan Li, Yuheng Li, and Yong Jae Lee. Improved baselines with visual instruction tuning. 2023. 1
- [47] Quanyu Long, Mingxuan Wang, and Lei Li. Generative imagination elevates machine translation. In *Proceedings of the 2021 Conference of the North American Chapter of the Association for Computational Linguistics: Human Language Technologies*, pages 5738–5748, 2021. 8
- [48] Yujie Lu, Wanrong Zhu, Xin Wang, Miguel Eckstein, and William Yang Wang. Imagination-augmented natural language understanding. In *Proceedings of the 2022 Conference of the North American Chapter of the Association for Computational Linguistics: Human Language Technologies*, pages 4392–4402, 2022. 4, 8
- [49] Yujie Lu, Pan Lu, Zhiyu Chen, Wanrong Zhu, Xin Eric Wang, and William Yang Wang. Multimodal procedural planning via dual text-image prompting. *arXiv preprint arXiv:2305.01795*, 2023. 8
- [50] Eran Malach and Shai Shalev-Shwartz. Decoupling “when to update” from “how to update”. *Advances in neural information processing systems*, 30, 2017. 8
- [51] David McAllester and Karl Stratos. Formal limitations on the measurement of mutual information. In *Proceedings of the Twenty Third International Conference on Artificial Intelligence and Statistics*, pages 875–884. PMLR, 2020. 3
- [52] Yu Meng, Jiaxin Huang, Yu Zhang, and Jiawei Han. Generating training data with language models: Towards zero-shot language understanding. *arXiv preprint arXiv:2202.04538*, 2022. 8
- [53] Yu Meng, Martin Michalski, Jiaxin Huang, Yu Zhang, Tarek Abdelzaher, and Jiawei Han. Tuning language models as training data generators for augmentation-enhanced few-shot learning. *arXiv preprint arXiv:2211.03044*, 2022. 8
- [54] Sergey I. Nikolenko. *Synthetic Data for Deep Learning*. Springer, 2021. 8
- [55] Ben Poole, Sherjil Ozair, Aaron Van Den Oord, Alex Alemi, and George Tucker. On variational bounds of mutual information. In *Proceedings of the 36th International Conference on Machine Learning*, pages 5171–5180. PMLR, 2019. 3
- [56] Zhenyue Qin, Dongwoo Kim, and Tom Gedeon. Neural network classifier as mutual information evaluator. In *International Conference on Machine Learning XAI Workshop*, 2020. 3
- [57] Alec Radford, Jong Wook Kim, Chris Hallacy, Aditya Ramesh, Gabriel Goh, Sandhini Agarwal, Girish Sastry, Amanda Askell, Pamela Mishkin, Jack Clark, et al. Learning transferable visual models from natural language supervision. In *International conference on machine learning*, pages 8748–8763. PMLR, 2021. 3
- [58] Aditya Ramesh, Prafulla Dhariwal, Alex Nichol, Casey Chu, and Mark Chen. Hierarchical text-conditional image generation with clip latents. *arXiv preprint arXiv:2204.06125*, 1(2):3, 2022. 1
- [59] Robin Rombach, Andreas Blattmann, Dominik Lorenz, Patrick Esser, and Björn Ommer. High-resolution image synthesis with latent diffusion models. In *Proceedings of the IEEE/CVF conference on computer vision and pattern recognition*, pages 10684–10695, 2022. 1, 5
- [60] Daniel Rose, Vaishnavi Himakunthala, Andy Ouyang, Ryan He, Alex Mei, Yujie Lu, Michael Saxon, Chinmay Sonar, Diba Mirza, and William Yang Wang. Visual chain of thought: Bridging logical gaps with multimodal infillings. *arXiv preprint arXiv:2305.02317*, 2023. 3, 8
- [61] Chitwan Saharia, William Chan, Saurabh Saxena, Lala Li, Jay Whang, Emily L Denton, Kamyar Ghasemipour, Raphael Gontijo Lopes, Burcu Karagol Ayan, Tim Salimans, et al. Photorealistic text-to-image diffusion models with deep language understanding. *Advances in Neural Information Processing Systems*, 35:36479–36494, 2022. 1
- [62] Katja Schwarz, Yiyi Liao, and Andreas Geiger. On the frequency bias of generative models. In *Advances in Neural Information Processing Systems*, pages 18126–18136. Curran Associates, Inc., 2021. 1, 5
- [63] Yanyao Shen and Sujay Sanghavi. Learning with bad training data via iterative trimmed loss minimization. In *International Conference on Machine Learning*, pages 5739–5748. PMLR, 2019. 8
- [64] Amanpreet Singh, Ronghang Hu, Vedanuj Goswami, Guillaume Couairon, Wojciech Galuba, Marcus Rohrbach, and Douwe Kiela. Flava: A foundational language and vision alignment model. In *Proceedings of the IEEE/CVF Conference on Computer Vision and Pattern Recognition*, pages 15638–15650, 2022. 1
- [65] Hwanjun Song, Minseok Kim, Dongmin Park, and Jae-Gil Lee. How does early stopping help generalization against label noise? *arXiv preprint arXiv:1911.08059*, 2019. 8
- [66] Hao Tan and Mohit Bansal. Vokenization: Improving language understanding with contextualized, visual-grounded supervision. *arXiv preprint arXiv:2010.06775*, 2020. 4, 8
- [67] Tianyi Tang, Yushuo Chen, Yifan Du, Junyi Li, Wayne Xin Zhao, and Ji-Rong Wen. Learning to imagine: Visually-augmented natural language generation. *arXiv preprint arXiv:2305.16944*, 2023. 3, 8
- [68] Naftali Tishby, Fernando C. Pereira, and William Bialek. The information bottleneck method. In *Proceedings of the 37-th Annual Allerton Conference on Communication, Control and Computing*, pages 368–377, 1999. 2
- [69] Jonathan Tremblay, Aayush Prakash, David Acuna, Mark Brophy, Varun Jampani, Cem Anil, Thang To, Eric Cameracci, Shaad Boochoon, and Stan Birchfield. Training deep networks with synthetic data: Bridging the reality gap by domain randomization. In *Proceedings of the IEEE Conference on Computer Vision and Pattern Recognition (CVPR) Workshops*, 2018. 8
- [70] Michael Tschannen, Josip Djolonga, Paul K. Rubenstein, Sylvain Gelly, and Mario Lucic. On mutual information

- maximization for representation learning. *ArXiv Preprint 1907.13625*, 2019. 3
- [71] Aäron van den Oord, Yazhe Li, and Oriol Vinyals. Representation learning with contrastive predictive coding. *ArXiv Preprint 1807.03748*, 2018. 3
- [72] Peng Wang, An Yang, Rui Men, Junyang Lin, Shuai Bai, Zhikang Li, Jianxin Ma, Chang Zhou, Jingren Zhou, and Hongxia Yang. Ofa: Unifying architectures, tasks, and modalities through a simple sequence-to-sequence learning framework. In *International Conference on Machine Learning*, pages 23318–23340. PMLR, 2022. 1
- [73] Xinyu Wang, Jiong Cai, Yong Jiang, Pengjun Xie, Kewei Tu, and Wei Lu. Named entity and relation extraction with multimodal retrieval. In *Findings of the Association for Computational Linguistics: EMNLP 2022*, pages 5925–5936, 2022. 6, 8, 3
- [74] Yizhong Wang, Yeganeh Kordi, Swaroop Mishra, Alisa Liu, Noah A Smith, Daniel Khashabi, and Hannaneh Hajishirzi. Self-instruct: Aligning language model with self generated instructions. *arXiv preprint arXiv:2212.10560*, 2022. 8
- [75] Zirui Wang, Jiahui Yu, Adams Wei Yu, Zihang Dai, Yulia Tsvetkov, and Yuan Cao. Simvln: Simple visual language model pretraining with weak supervision. *arXiv preprint arXiv:2108.10904*, 2021. 1
- [76] Peter West, Chandra Bhagavatula, Jack Hessel, Jena D Hwang, Liwei Jiang, Ronan Le Bras, Ximing Lu, Sean Welleck, and Yejin Choi. Symbolic knowledge distillation: from general language models to commonsense models. *arXiv preprint arXiv:2110.07178*, 2021. 8
- [77] Shengqiong Wu, Hao Fei, Yixin Cao, Lidong Bing, and Tat-Seng Chua. Information screening whilst exploiting! multimodal relation extraction with feature denoising and multimodal topic modeling. *arXiv preprint arXiv:2305.11719*, 2023. 6, 8, 3
- [78] Zhao Xiaoyan, Deng Yang, Yang Min, Wang Lingzhi, Zhang Rui, Cheng Hong, Lam Wai, Shen Ying, and Xu Ruifeng. A comprehensive survey on deep learning for relation extraction: Recent advances and new frontiers. *arXiv preprint arXiv:2306.02051*, 2023. 1
- [79] Bo Xu, Shizhou Huang, Ming Du, Hongya Wang, Hui Song, Yanghua Xiao, and Xin Lin. A unified visual prompt tuning framework with mixture-of-experts for multimodal information extraction. In *International Conference on Database Systems for Advanced Applications*, pages 544–554. Springer, 2023. 6
- [80] Zhaohui Yan, Zixia Jia, and Kewei Tu. An empirical study of pipeline vs. joint approaches to entity and relation extraction. In *Proceedings of the 2nd Conference of the Asia-Pacific Chapter of the Association for Computational Linguistics and the 12th International Joint Conference on Natural Language Processing*, pages 437–443, 2022. 1
- [81] Yue Yang, Wenlin Yao, Hongming Zhang, Xiaoyang Wang, Dong Yu, and Jianshu Chen. Z-lavi: Zero-shot language solver fueled by visual imagination. In *Proceedings of the 2022 Conference on Empirical Methods in Natural Language Processing*, pages 1186–1203, 2022. 3, 8
- [82] Quanming Yao, Hansi Yang, Bo Han, Gang Niu, and James Tin-Yau Kwok. Searching to exploit memorization effect in learning with noisy labels. In *International Conference on Machine Learning*, pages 10789–10798. PMLR, 2020. 8
- [83] Jiacheng Ye, Jiahui Gao, Qintong Li, Hang Xu, Jiangtao Feng, Zhiyong Wu, Tao Yu, and Lingpeng Kong. Zerogen: Efficient zero-shot learning via dataset generation. *arXiv preprint arXiv:2202.07922*, 2022. 8
- [84] Moon Ye-Bin, Nam Hyeon-Woo, Wonseok Choi, Nayeong Kim, Suha Kwak, and Tae-Hyun Oh. Synaug: Exploiting synthetic data for data imbalance problems. *arXiv Preprint 2308.00994*, 2023. 8
- [85] Jianfei Yu, Jing Jiang, Li Yang, and Rui Xia. Improving multimodal named entity recognition via entity span detection with unified multimodal transformer. Association for Computational Linguistics, 2020. 6, 8
- [86] Xingrui Yu, Bo Han, Jiangchao Yao, Gang Niu, Ivor Tsang, and Masashi Sugiyama. How does disagreement help generalization against label corruption? In *International Conference on Machine Learning*, pages 7164–7173. PMLR, 2019. 8
- [87] Li Yuan, Yi Cai, Jin Wang, and Qing Li. Joint multimodal entity-relation extraction based on edge-enhanced graph alignment network and word-pair relation tagging. In *Proceedings of the AAAI conference on artificial intelligence*, pages 11051–11059, 2023. 8
- [88] Daojian Zeng, Haoran Zhang, and Qianying Liu. Copymtl: Copy mechanism for joint extraction of entities and relations with multi-task learning. In *Proceedings of the AAAI conference on artificial intelligence*, pages 9507–9514, 2020. 1
- [89] Dong Zhang, Suzhong Wei, Shoushan Li, Hanqian Wu, Qiaoming Zhu, and Guodong Zhou. Multi-modal graph fusion for named entity recognition with targeted visual guidance. In *Proceedings of the AAAI conference on artificial intelligence*, pages 14347–14355, 2021. 6, 8
- [90] Lvmin Zhang, Anyi Rao, and Maneesh Agrawala. Adding conditional control to text-to-image diffusion models. In *Proceedings of the IEEE/CVF International Conference on Computer Vision*, pages 3836–3847, 2023. 1
- [91] Pengchuan Zhang, Xiujun Li, Xiaowei Hu, Jianwei Yang, Lei Zhang, Lijuan Wang, Yejin Choi, and Jianfeng Gao. Vinvl: Revisiting visual representations in vision-language models. In *Proceedings of the IEEE/CVF conference on computer vision and pattern recognition*, pages 5579–5588, 2021. 1
- [92] Shiyue Zhang and Mohit Bansal. Addressing semantic drift in question generation for semi-supervised question answering. In *Proceedings of the 2019 Conference on Empirical Methods in Natural Language Processing and the 9th International Joint Conference on Natural Language Processing (EMNLP-IJCNLP)*, pages 2495–2509, Hong Kong, China, 2019. Association for Computational Linguistics. 3
- [93] Qihui Zhao, Tianhan Gao, and Nan Guo. Tsvfn: Two-stage visual fusion network for multimodal relation extraction. *Information Processing & Management*, 60(3):103264, 2023. 1, 6, 8
- [94] Changmeng Zheng, Junhao Feng, Ze Fu, Yi Cai, Qing Li, and Tao Wang. Multimodal relation extraction with efficient graph alignment. In *Proceedings of the 29th ACM Interna-*

tional Conference on Multimedia, pages 5298–5306, 2021. 6, 8, 3

- [95] Changmeng Zheng, Zhiwei Wu, Junhao Feng, Ze Fu, and Yi Cai. MNRE: A challenge multimodal dataset for neural relation extraction with visual evidence in social media posts. In *2021 IEEE International Conference on Multimedia and Expo (ICME)*, pages 1–6. IEEE, 2021. 1, 5, 6, 8
- [96] Changmeng Zheng, Junhao Feng, Yi Cai, Xiaoyong Wei, and Qing Li. Rethinking multimodal entity and relation extraction from a translation point of view. In *Proceedings of the 61st Annual Meeting of the Association for Computational Linguistics (Volume 1: Long Papers)*, Toronto, Canada, 2023. 2, 6, 8, 3
- [97] Wanrong Zhu, An Yan, Yujie Lu, Wenda Xu, Xin Wang, Miguel Eckstein, and William Yang Wang. Visualize before you write: Imagination-guided open-ended text generation. In *Findings of the Association for Computational Linguistics: EACL 2023*, pages 78–92, 2023. 8

Training on Synthetic Data Beats Real Data in Multimodal Relation Extraction

Supplementary Material

7. Mathematical Details

7.1. Proposition 1

We have two random variables, input X and a discrete label Y . Y can take on M values with equal probability. f is an arbitrary neural network whose output are not necessarily normalized. We would like to show

$$I(X, Y) \geq \mathbb{E}_{X, Y} \left[\log \frac{\exp f(x, y)}{\sum_{y'} [\exp f(x, y')]} \right]. \quad (7)$$

Proof.

$$I(X, Y) = \mathbb{E}_{X, Y} \left[\log \frac{P(X, Y)}{P(X)P(Y)} \right] \quad (8)$$

$$= \mathbb{E}_{X, Y} \left[\log \left(\frac{Q(X, Y) P(X, Y)}{P(X)P(Y) Q(X, Y)} \right) \right] \quad (9)$$

$$= \mathbb{E}_{X, Y} \left[\log \frac{Q(X, Y)}{P(X)P(Y)} \right] + \mathbb{E}_{X, Y} \left[\log \frac{P(X, Y)}{Q(X, Y)} \right] \quad (10)$$

$$= \mathbb{E}_{X, Y} \left[\log \frac{Q(X, Y)}{P(X)P(Y)} \right] + KL[P(X, Y) \| Q(X, Y)] \quad (11)$$

$$\geq \mathbb{E}_{X, Y} \left[\log \frac{Q(X, Y)}{P(X)P(Y)} \right] \quad (12)$$

Here $Q(X, Y)$ is an arbitrary distribution. To ensure it is a valid distribution, we let

$$Q(X = x, Y = y) = \frac{P(x)P(y) \exp(f_\theta(x, y))}{\mathbb{E}_{y'} [\exp(f_\theta(x, y'))]} \quad (13)$$

We can easily verify that

$$\int_{-\infty}^{\infty} Q(X = x, Y = y) dx dy = 1 \quad (14)$$

Substituting Eq. 13 back to Eq. 12, we obtain

$$I(X, Y) \geq \mathbb{E}_{X, Y} \left[\log \frac{\exp f(x, y)}{\mathbb{E}_{y'} [\exp f(x, y')]} \right] \quad (15)$$

$$= \mathbb{E}_{X, Y} \left[\log \frac{\exp f(x, y)}{\frac{1}{M} \sum_{y'} [\exp f(x, y')]} \right] \quad (16)$$

$$= \mathbb{E}_{X, Y} \left[\log \frac{\exp f(x, y)}{\sum_{y'} [\exp f(x, y')]} \right] + \log M \quad (17)$$

$$\geq \mathbb{E}_{X, Y} \left[\log \frac{\exp f(x, y)}{\sum_{y'} [\exp f(x, y')]} \right] \quad \square \quad (18)$$

7.2. Proposition 2

Suppose we have a sequence of random variables X_1, X_2, \dots, X_N and they form a Markov chain. In other words, for all integer M , X_i and X_{i+M} are independent given $X_{i+m}, \forall 1 \leq m \leq M - 1$. We want to prove that the mutual information $I(X_1; X_N) \leq I(X_i, X_j), \forall 1 < i < j \leq N$.

Proof. First, consider X_1, X_i and $X_N, i < N$. By the chain rule of mutual information,

$$\begin{aligned} I(X_1 X_i; X_N) &= I(X_1; X_N) + I(X_i; X_N | X_1) \\ &= I(X_i; X_N) + I(X_1; X_N | X_i) \end{aligned} \quad (19)$$

Since X_1 and X_N are independent given X_i , $I(X_1; X_N | X_i) = 0$.

$$I(X_1; X_N) = I(X_i; X_N) - I(X_i; X_N | X_1) \leq I(X_i; X_N) \quad (20)$$

Next, we consider $I(X_N X_j; X_i), i < j < N$. By the same logic as above,

$$I(X_i; X_N) \leq I(X_i; X_j), \forall i < j < N. \quad (21)$$

This completes the proof. \square

8. Diversity Estimates

Data diversity is inherently difficult to define because simple statistics may not correspond well to semantic diversity. As an approximate measure, we use the generalized variance of a Gaussian mixture model (GMM) fitted on synthetic data. First, we extract a feature vector from each synthetic sample using a pretrained neural network. We use CLIP-ViT-B-32 as the image encoder and BERT-base-uncased as the text encoder. As the data lie in a low-dimensional manifold, we apply principal component analysis (PCA) to reduce the feature dimension to D_{PCA} . Second, we fit a GMM, which contains N Gaussian distributions with mean \mathbf{u}_i and diagonal covariance matrix Σ_i .

To calculate the variance of the GMM, we apply the law of total variance. Let random variable C denote the component that a data point X belongs to, we have

$$\begin{aligned} \text{Var}(X) &= \mathbb{E}[\text{Var}(X|C)] + \text{Var}(\mathbb{E}[X|C]) \\ &= \sum_i^N p_i \Sigma_i + \sum_i^N p_i (\mathbf{u}_i - \bar{\mathbf{u}})(\mathbf{u}_i - \bar{\mathbf{u}})^\top, \end{aligned} \quad (22)$$

since $\text{Var}(X|C = i) = \Sigma_i$ and $\mathbb{E}_X[X|C = i] = \mathbf{u}_i$. $\bar{\mathbf{u}} = \sum_i^N p_i \mathbf{u}_i$. We use generalized variance, which is the

Table 5. Evaluation of the diversity on various synthetic sets.

	D_{PCA}	N	V_0	V'_1	V_1	V'_2	
Image	16	1	1.06×10^{13}	1.42×10^{13} (+33.96%)	9.98×10^{12}	1.51×10^{13} (+51.30%)	
		3	9.12×10^{12}	1.20×10^{13} (+31.58%)	8.69×10^{12}	1.32×10^{13} (+51.90%)	
		5	7.11×10^{12}	1.15×10^{13} (+61.74%)	6.71×10^{12}	1.17×10^{13} (+74.37%)	
	32	1	9.12×10^{21}	9.36×10^{21} (+2.63%)	6.47×10^{21}	9.55×10^{21} (+47.60%)	
		3	6.95×10^{21}	7.37×10^{21} (+6.04%)	5.52×10^{21}	7.37×10^{21} (+33.51%)	
		5	5.95×10^{21}	6.74×10^{21} (+13.28%)	4.57×10^{21}	7.12×10^{21} (+55.80%)	
	64	1	3.08×10^{34}	1.47×10^{34} (-52.27%)	1.23×10^{34}	1.41×10^{34} (+14.63%)	
		3	2.32×10^{34}	1.24×10^{34} (-46.55%)	1.01×10^{34}	1.18×10^{34} (+16.83%)	
		5	2.17×10^{34}	1.03×10^{34} (-52.53%)	8.68×10^{33}	9.58×10^{33} (+10.37%)	
	Text	16	1	6.43×10^{20}	8.75×10^{20} (+36.08%)	8.38×10^{20}	1.00×10^{21} (+19.33%)
			3	5.75×10^{20}	7.77×10^{20} (+35.13%)	7.45×10^{20}	9.06×10^{20} (+21.61%)
			5	5.81×10^{20}	7.53×10^{20} (+29.60%)	7.39×10^{20}	8.72×10^{20} (+18.00%)
32		1	2.17×10^{32}	3.86×10^{32} (+77.88%)	3.57×10^{32}	4.22×10^{32} (+18.21%)	
		3	1.85×10^{32}	3.28×10^{32} (+77.30%)	3.04×10^{32}	3.71×10^{32} (+22.04%)	
		5	1.74×10^{32}	2.86×10^{32} (+64.37%)	2.91×10^{32}	3.43×10^{32} (+17.87%)	
64		1	2.45×10^{43}	1.06×10^{44} (+332.65%)	1.02×10^{44}	7.96×10^{43} (-21.96%)	
		3	2.04×10^{43}	8.68×10^{43} (+325.49%)	8.57×10^{43}	6.49×10^{43} (-24.27%)	
		5	1.85×10^{43}	7.84×10^{43} (+323.78%)	7.43×10^{43}	5.94×10^{43} (-20.05%)	

determinant of the covariance matrix.

$$\sigma^2 = \det \left(\sum_i^N p_i \Sigma_i + \sum_i^N p_i (\mathbf{u}_i - \bar{\mathbf{u}})(\mathbf{u}_i - \bar{\mathbf{u}})^\top \right) \quad (23)$$

In Table 5, we present the variance results in two CCG steps using different numbers of GMM components and feature dimensions. Across different choices of GMM components, we consistently observe that variance increases with each generation step when D_{PCA} is 16 or 32. However, when the $D_{\text{PCA}} = 64$, this trend does not always hold true. We argue that this shows CCG increases variance on the most important principal components of the feature space. Variations in the less important principal directions are likely less recognizable by humans and could be considered as noise. Examples of such variations are changes in the blurred image regions or textures of grass and tree leaves. Though humans tend to ignore such details, they contribute to the variance nonetheless. However, such details probably do not contribute significantly toward representation learning of the student network.

9. Implementation Details

9.1. Experiments on MNRE

During training of the student and teacher, the optimizer and learning rate scheduler is AdamW and Cosine Decay. The student adopts a learning rate of 10^{-5} , a batch size of 16, and a weight decay of 10^{-2} , while the teacher employs a batch size of 256 and a weight decay of 10^{-2} . The learning

rate of the teacher is set to 3×10^{-7} and 5×10^{-7} when training on synthetic texts and images, respectively.

Data augmentation is applied to real data during student training to mitigate overfitting. For the real texts, we randomly select 30% tokens excluding the entity pair. Then, we mask them with the probability of 0.8, or replace them with a random token in the vocabulary with the probability of 0.2. For the real images, we apply the RandAugment [10], where the number of augmentation transformations and the magnitude for transformations is 2 and 7, respectively.

9.2. Experiments on WebNLG

We set the number of Chained Cross-modal Generation (CCG) iterations, denoted as K , to 1. For each real text in U_0 , we generate 10 synthetic images for V'_0 . After the teacher network selects 60% images (i.e., 6 images), the first CCG round generates 24 synthetic views, providing 4 new images for each input. At last, we choose 4 synthetic images for each real text during student training.

In the student model, we adopt a learning rate of 5×10^{-5} , a batch size of 16, and a weight decay of 10^{-2} . For the teacher model, we use a learning rate of 7×10^{-6} , a batch size of 128, and a weight decay of 10^{-2} . To address potential overfitting issues, we implement the same text augmentation as used in MNRE.

Table 6. Statistics of MNRE and WebNLG

Statistics	MNRE	WebNLG
# Word	258k	290k
# Sentence	9,201	6,222
# Words Per Sentence	28	47
# Instance	15,485	14,485
# Entity	30,970	28,970
# Relation	23	171
# Image	9,201	-

10. Dataset Statistics

The statistics of the multimodal dataset MNRE compared with the textual dataset WebNLG are listed in Tab. 6. Sentences in WebNLG contain 68% more words than those in MNRE. This difference in text length suggests sentences in WebNLG are not easily visualized, potentially reducing the advantage of the multimodal classifier.

11. Baselines in Main Results

We compare MI²RAGE against 19 baselines for the multimodal relation extraction. It is noted that all of them are trained on real multimodal data. Here we give more details.

The methods in the first category leverage a large number of image-text pairs. TMR [96] and [29] additionally leverage 400k and 988k unlabeled image-caption pairs, respectively. In addition, TMR [96] utilizes text-to-image generation, employing real text and generated images for multi-grained representation learning. In the second category, image and text retrieval is employed. For example, MoRe [73] and [30] enhance their datasets by retrieving additional images and texts from Wikipedia and Google, respectively. GPT4-XMLR [6] retrieves textual information from large language models to train a compact student model.

Other works can be further categorized into two groups. In the first group, MRE-ISE [77] and MEGA [94] utilize pretrained scene graph extraction models, employing graph neural networks to obtain multimodal graph representations for structural alignment. In the second group, HVPNet [9], DGF-PT [43], I²SRM [31], Iformer [40], and RECK [14] integrate pretrained object detectors to achieve fine-grained alignment between textual tokens and visual objects.

12. Comparison Against Test-time Data Augmentation

In this section, we compare our proposed method with a similar approach, test-time data augmentation (TDA), which also leverages multiple different images as an ensemble during inference. Specifically, the model takes one image-text pair at a time and is trained on real data in MNRE. During inference, we use RandAugment [10] on

Table 7. Experimental results of test-time data augmentation. There are two hyperparameters λ_1 and λ_2 in the RandAugment. λ_1 represents the number of augmentation transformations to apply sequentially, while λ_2 corresponds to the magnitude for all the transformations in the sequence.

Method	Accuracy	Precision	Recall	F1
MI ² RAGE	96.65	93.92	91.72	92.81
No TDA	76.77	65.63	65.94	65.78
$\lambda_1=1, \lambda_2=3$	76.64	65.67	65.47	65.57
$\lambda_1=2, \lambda_2=5$	76.58	65.87	64.84	65.35
$\lambda_1=3, \lambda_2=7$	76.64	65.77	65.16	65.46
$\lambda_1=4, \lambda_2=9$	76.58	65.97	64.53	65.24

the real image and randomly obtain N augmented images. We collect these synthetic images and the real images into an image pool. Subsequently, we feed the real text and one image from the pool to the model at a time, yielding $N + 1$ probability vectors, which are averaged for the final prediction. The label with the highest probability is chosen as the ensemble prediction. We set N to 6, the same as the student network in MI²RAGE. The results are presented in Table 7. We observe that TDA does not yield performance gain and even marginally decreases performance.

13. Examples of cross-modality generation

We give more synthetic examples in Fig. 6 and 7. We can observe that the synthetic data generated in CCG is more diverse compared to those directly generated from real data.




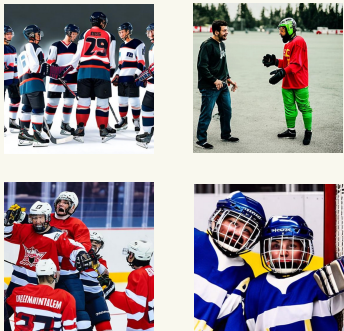


Real Text & Entity Pair	Synthetic Images in V'_0	Synthetic Images in CCG	Relation Label
<p>The year is 2038. 58 year old Rafa Nadal has won The French Open again.</p>			Awarded
<p>Stamkos and Malkin dropping is what makes hockey so great. Two superstars just chuckin knucks.</p>			Peer
<p>Fouad al Mohandes and his twin brother Sami al Mohandes.</p>			Sibling

Figure 6. Examples of generated images when the real image are missing. We show the images in V'_0 which is directly generated from the real text by text-to-image generation. In addition, we give some synthetic samples in the Chained Cross-modality Generation (CCG).

Real Image & Entity Pair**Synthetic Texts****Relation Label**

Piolo Pascual

Arci Munoz

Synthetic Texts in V'_0

a couple sitting next to each other kissing on a table
 a young woman who is sitting next to a man who is kissing her cheek
 young couple in a restaurant sharing a big smile for camera
 a man and woman in striped shirts sharing an affection

Synthetic Texts in CCG

the newly married couple sharing a moment after their wedding
 two men are kissing and embracing in a room
 a man and woman sharing an intimate moment at a wooden table
 man kissing his girlfriend with a soft kiss on cheek

Couple



Kobe Bryant

NBA MVP

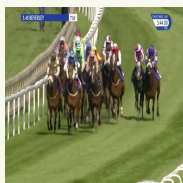
Synthetic Texts in V'_0

a man holding up a trophy
 a man holding a trophy wearing lakers uniforms
 a man giving a hand sign with another hand
 a couple of men standing on top of a court holding an trophy

Synthetic Texts in CCG

a basketball player dribbling the basketball in front of a crowd
 a man holding a trophy wearing a lakers uniform and suit
 a man holding a trophy and looking up while wearing a jersey
 an image of kobe's incredible moment of fame with the lakers

Awarded



Nature Boy

Leconfield Handicap

Synthetic Texts in V'_0

a close up of several horses racing across the course
 a row of horses that are running on a track
 several jockeys are racing horses on the track
 a group of people are racing horses across a field

Synthetic Texts in CCG

a basketball player dribbling the basketball in front of a crowd
 two jockeys and a horse race in motion
 a jockey riding a brown horse around a ramp
 a person riding a horse on a grassy race track

Race

Figure 7. Examples of generated captions when the real text are missing. We present the captions in V'_0 which is directly generated from the real image by image-to-text generation. Besides, we show some synthetic caption in the Chained Cross-modality Generation (CCG).